



## CONSTRUCTION AND CHARACTERIZATION OF A NANOSTRUCTURED BIOCATALYST CONSISTING OF IMMOBILIZED LIPASE ON Mg-AMINO-CLAY

MINGZHU ZHANG<sup>1</sup>, SHIYONG SUN<sup>1</sup>\* , RUI LV<sup>1</sup>, YEVGENY ALEKSANDROVICH GOLUBEV<sup>2</sup>,  
KE WANG<sup>1</sup>, FAQIN DONG<sup>1</sup>, OLGA BORISOVNA KOTOVA<sup>2</sup>, AND ELENA LEONIDOVNA KOTOVA<sup>3</sup>

<sup>1</sup>Institute of Non-metallic Minerals, Key Laboratory of Solid Waste Treatment and Resource Recycle of Ministry of Education, School of Environment and Resource, Southwest University of Science and Technology, Mianyang 621000, China

<sup>2</sup>Yushkin's Institute of Geology, Komi Science Center, Ural Branch of RAS, ul. Pervomayskaya, 54, 167982 Syktyvkar, Russia

<sup>3</sup>Mining State University St. Petersburg, 21st Line, 199106 St. Petersburg, Russia

**Abstract**—Lipase is an industrial enzyme, the catalytic efficiency of which is restricted by various environmental factors. To improve this efficiency, immobilization technology has been utilized in the past to improve the stability of lipase in harsh conditions. Immobilization technology can be divided into physical methods and chemical methods. Some unsolved problems remain in current immobilization technology. The interaction between enzyme and immobilization support is weak and reversible during physical adsorption, resulting in poor stability of the immobilized enzyme and the contamination of substrate solution by leached enzymes. In chemical methods, enzyme-active sites might be inactivated due to the chemical reactions between enzyme molecules and support, resulting in a decrease in the enzymes' catalytic activity (Liu et al., 2018a). The objective of the current study was to construct a nanostructured lipase via Mg-amino-clay as a carrier and improve the catalytic activity and stability of lipase by immobilization. Lipase produced by *Aspergillus oryzae* was immobilized on aminopropyl functionalized magnesium phyllosilicate (a 2:1 trioctahedral talc-like silicate Mg-amino-clay) via a 1-(3-Dimethylaminopropyl)-3-ethyl-carbodiimide hydrochloride (EDC) coupling agent. The physical and chemical properties of the Mg-amino-clay and Mg-amino-clay-based nanostructured biocatalyst (Mg-clay-lipase) were characterized by X-ray diffraction, Fourier-transform infrared spectroscopy, and scanning electron microscopy. Optimal immobilization conditions were determined by taking into account the following variables: amount of initial lipase, EDC concentration, and reaction time. The results revealed that the optimum temperature, pH, and thermal stability of Mg-clay-lipase were greater than equivalent values for free lipase under optimal conditions (described below – *Process for Immobilization of Lipase on Mg-amino-clay*). The Michaelis-Menten constant ( $K_m$ ) values were 5.25 mM and 7.42 mM while the maximum reaction rates ( $v_{max}$ ) were 30.58 mM/(L·min) and 55.87 mM/(L·min) for free lipase and Mg-clay-lipase, respectively. The present study provided a new nanostructured biocatalyst and demonstrated that the enzyme activity and stability of Mg-clay-lipase were superior to those of free lipase due to the mechanism of 'interface activation'.

**Keywords**—Biocatalyst · Enzyme immobilization · Lipase · Mg-amino-clay

### INTRODUCTION

Enzymes are efficient biocatalysts which enhance the reaction rates of various biological and chemical processes (Madhavan et al., 2017). Lipase (EC 3.1.1.3) is one of the most important industrial enzymes and has the ability to catalyze a wide range of reactions in non-aqueous and aqueous environments (Aghaei et al., 2020), e.g. hydrolysis (Akash & Weatherley, 2018; Atiroğlu, 2020; Urrutia et al., 2018), acidolysis (de Paula et al., 2018; Kavadia et al., 2018), transesterification (Kołodziejska et al., 2018; Löfgren et al., 2019; Wijnants et al., 2018), and esterification (Barse et al., 2019; de Barros et al., 2019; Papadaki et al., 2018). Some lipase properties are often unavailable for industrial applications because the catalytic efficiency and stability of natural lipase are limited by various environmental factors, including high temperature, extreme pH (strong acid or alkaline), high

salinity, and organic solvents (Madhavan et al., 2017). Immobilization has proven to be a powerful tool to improve many features of lipase and to solve the problems of recovery and stability which have limited the application of enzymes as industrial catalysts (Urrutia et al., 2018). The interfacial activation of lipase is a key factor in lipase immobilization. As reported by Brzozowski et al. (1991), the active center of the lipase molecule is covered by a movable region known as the "lid." When lipase is adsorbed on the hydrophobic supports, the hydrophobic microenvironment on the carrier exposes the lid completely (Manoel et al., 2015), causing improvement in enzymatic activity.

Various methods have been proposed for the immobilization of lipase. The main strategies can be divided into physical methods and chemical methods. The physical methods include adsorption and entrapment in which the interaction between matrix and enzyme is weak, but the conformation of the enzyme can be retained (Sheldon, 2007). The chemical methods refer to the immobilization of the enzyme on the modified support via covalent binding or cross-linking (Hanefeld et al., 2009). Sometimes, functional groups on the support material are activated by certain reagents to provide multipoint sites for the enzyme, which improves its stability.

The paper is based on a presentation made during the 4th Asian Clay Conference, Thailand, June 2020.

\* E-mail address of corresponding author: shysun@swust.edu.cn  
DOI: 10.1007/s42860-021-00130-z

© The Clay Minerals Society 2021

The immobilization of the enzyme not only improves its stability, but also its catalytic activity, and also reduces its inhibition by substrates or products. These advantages depend on the lipase itself, on the immobilization technique, and on the support (Cipolatti et al., 2017; Fernandez-Lafuente et al., 1998; Palomo et al., 2007). Among these, the support is an important factor in determining the effectiveness of the immobilized enzyme. Immobilization of lipase on hydrophobic supports has been attributed to the interfacial activation of the lipase vs the support surface (Fernandez-Lafuente et al., 1998). As a general rule, a more hydrophobic support may immobilize more lipase than a less hydrophobic one.

The ideal support for enzyme immobilization should have excellent biocompatibility, stable physical and chemical properties, and abundant binding sites for the enzyme (Hartmann & Kostrov, 2013). The most commonly employed supports include nanofibers, polymeric monoliths, mesoporous materials, nanomaterials, membranes, and cellulose paper. In recent years, nano-materials have provided new opportunities for the construction of nanostructured enzyme catalysts due to their large specific surface area, significant surface reactivity, and great mechanical strength (Wang et al., 2019). Previous research suggested that the *Candida antarctica* lipase B (CALB) immobilized on poly (glycidyl methacrylate-co-methylacrylate)/feather polypeptide (P(GMA-coMA)/FP) nanofibrous membranes that contain reactive epoxy groups and biocompatible FP preserved ~38% of the catalytic activity after treatment at 70°C for 3 h (Liu et al., 2018a, b). Another study (Wang et al., 2016) showed that a magnetic support consisting of carboxyl-functionalized Fe<sub>3</sub>O<sub>4</sub> nanorods and MIL-100 (Fe) was employed to immobilize *Candida rugosa* lipase (CRL), and ~60% of the initial activity of CRL was retained even after ten reaction cycles (Wang et al. 2016). New functional materials integrating the benefits of large porosity, simple operation, tunable morphology, and ultra-large surface area:volume ratios are anticipated.

The amino organophyllosilicates (amino-clays), which belong to the family of inorganic-organic hybrid materials, possess an array of organic moieties within an inorganic matrix to form a 2:1 trioctahedral talc-like structure (Burkett et al., 1997). The prime advantage of amino-clay is that it offers free and reversible exfoliation in water by protonation, but reverts easily to the stacked form by the addition of less-polar solvents such as ethanol (Datta et al., 2013). Amino-clay has been employed widely, therefore, as a carrier for the immobilization of biomolecules including DNA (Patil et al., 2007), protein (myoglobin, haemoglobin), glucose oxidase (Patil et al., 2005), and anti-inflammatory drugs (ibuprofen, antioxidant polyphenol, and epigallocatechin) (Holmström et al., 2007). A previous study showed that the stabilities of the intercalated DNA and immobilized enzyme at elevated temperatures over a wide range of pH were improved significantly (Holmström et al., 2007). The catalytic efficiency of free lipase is very strict for pH, temperature, high salinity, etc. The aim of the current study was to improve the catalytic performance and stability of lipase by constructing a nanostructured lipase via Mg-amino-clay as a carrier.

## MATERIALS AND METHODS

### Materials and Reagents

Lipase (from *A. oryzae*, lyophilized powder), bovine serum albumin (BSA), p-nitrophenyl phosphate (p-NPP), p-nitrophenol (p-NP), and 1-(3-Dimethylaminopropyl)-3-ethyl-carbodiimide hydrochloride (EDC) were supplied by Aladdin Industrial Corp. (Shanghai, China). 3-aminopropyltriethoxysilane (APTES) was purchased from Macklin Biochemical Co., Ltd. (Shanghai, China). All other chemicals, such as anhydrous ethanol, MgCl<sub>2</sub>·6H<sub>2</sub>O, Coomassie Brilliant Blue G-250, and tris (hydroxymethyl) methyl aminomethane hydrochloride (Tris-HCl) were acquired from Chengdu Kelon Chemical Reagent Company (Chengdu, China).

### Characterization

The morphology of the samples (Mg-amino-clay, Mg-clay-lipase) was characterized by scanning electron microscopy (SEM) (Sigma300, Carl Zeiss, Jena, Germany), where samples were mounted on double-sided adhesive tape and sputter coated with 5–10 nm of gold prior to imaging at an accelerating voltage of 5 kV. Mineralogy was determined by X-ray diffraction (XRD) (Ultima IV with D/teX Ultra, Rigaku, Tokyo, Japan) with a small-angle accessory from 2 to 25°2θ using CuKα radiation ( $\lambda = 1.5406 \text{ \AA}$ , 40 kV, 30 mA). Fourier-transform infrared (FTIR) spectra of KBr pressed pellets (sample:KBr ratio of 1:100) were recorded using a (Perkin Elmer) Spectrum One instrument (Waltham, Massachusetts, USA) in the spectral range of 4000–400 cm<sup>-1</sup> at a resolution of 4 cm<sup>-1</sup>. The zeta ( $\zeta$ ) potential was measured using a Zetasizer Nano ZS 90 (Malvern Instruments, Malvern, Worcestershire, UK). The UV-Vis absorption spectra were collected using a NanoDrop 2000C spectrophotometer (Thermo Scientific, Waltham, Massachusetts, USA).

### Preparation of Mg-amino-clay

Ethanol (20 mL) was used to dissolve 8.4 g of MgCl<sub>2</sub>·6H<sub>2</sub>O (41.32 mmol), stirring at room temperature. 13 mL (58.73 mmol) of 3-aminopropyltriethoxysilane (APTES) was then added, drop-wise, with continuous stirring in a shaker. A white suspension was formed after several minutes, and stirring was continued overnight. The resulting products were centrifuged, washed with ethanol, and dried at 40°C. The white solid was then ground to produce a powder (Park et al., 2018).

### Lipase Immobilization

To prepare Mg-clay-lipase, 0.1 g of Mg-amino-clay was reacted with 20 mL of a solution of EDC (0.4 g/L) in a phosphate buffer for 1 h at room temperature. In order to eliminate the remaining EDC, the precipitate was centrifuged and washed twice with a phosphate buffer (pH 7.0). After this, 0.1 g of the support was introduced into the solution of lipase (2.5 mg/mL), stirring for 3 h. The product was washed carefully with a phosphate buffer several times until all unbound lipase was removed and then used directly for the lipase activity measurements. The immobilization procedure is illustrated in Fig. 1.

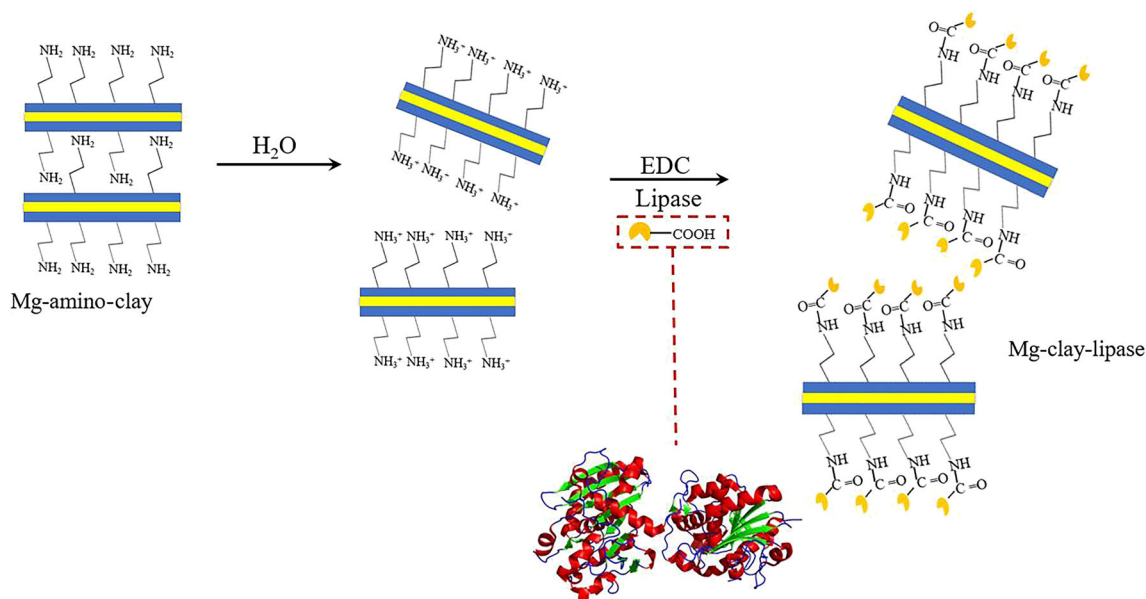


**Fig. 1.** Schematic diagram of Mg-amino-clay dispersed in water and lipase immobilization on Mg-amino-clay

#### Lipase Assay

The Bradford method was used to determine the amount of lipase loaded using BSA as a standard (Bradford, 1976). The amount of bound lipase was calculated indirectly by the difference between the lipase remaining in the supernatants and the amount of lipase loaded (Öztürk et al., 2016). The lipase immobilization efficiency is given in Eq. 1.

$$\text{Immobilization efficiency (\%)} = \frac{M_0 - M_1}{M_0} \times 100 \quad (1)$$

where  $M_0$  is the initial concentration of lipase solution and  $M_1$  is the final unbound lipase concentration in the supernatant after immobilization.

#### Lipase Activity Assay

Hydrolysis of the p-nitrophenyl palmitate was investigated using a colorimetric method, as follows. The enzymatic activities of free lipase and Mg-clay-lipase were tested by hydrolysis of p-NPP (10 mM in 2-propanol) in Tris-HCl buffer (100 mM, pH 9) (Gupta et al., 2005). The reaction was initiated by adding free/immobilized lipase and incubated for 10 min at room temperature. The absorbance of the product (p-NP) was measured at 410 nm. Spontaneous hydrolysis of p-NPP was also considered using a blank, i.e. without lipase, as a control (Badoei-dalfard et al., 2019). One unit (U) of lipase was defined as the amount of enzyme that liberates one micromole of p-nitro phenol per minute under the assay conditions.

#### Kinetic Analysis

The dependence of enzyme activity on substrate concentration for the immobilized lipase on nanocomposites was evaluated by Michaelis-Menten (M-M) kinetics using Eq. 2. The kinetics of the free lipase and Mg-clay-lipase were studied

by adding p-NPP as the substrate with increasing concentrations ranging from 0.2 to 4.0 mM.

$$v = \frac{v_{\max} S}{K_m + S} \quad (2)$$

where  $v_{\max}$  is the greatest possible specific lipase activity ( $\text{U g}^{-1}$ ),  $S$  is the concentration of substrate, and  $K_m$  is the Michaelis-Menten (M-M) constant (mM) determined from the substrate concentration that gives a specific lipase activity of  $\frac{1}{2}v_{\max}$ . The kinetics of free lipase and Mg-clay-lipase were assayed for  $K_m$  and the maximum reaction rate ( $v_{\max}$ ), which were calculated from Lineweaver-Burk (Eq. 3) plots using the initial rate of the reaction,  $v_0$ , in which  $S_0$  is the initial substrate concentration.

$$\frac{1}{v_0} = \left( \frac{1}{v_{\max}} \right) + \left( \frac{K_m}{v_{\max}} \right) \left( \frac{1}{S_0} \right) \quad (3)$$

## RESULTS AND DISCUSSION

#### Characterization

**SEM analysis.** The micromorphologies of the various systems were examined to determine the structure and surface properties of the clay minerals. Scanning electron microscopy of the Mg-amino-clay (Fig. 2a) indicated that its morphology was of a uniformly layered structure, and the higher resolution image (Fig. 2b) showed lipase particles attached to a support, possibly by covalent immobilization, indicating that the lipase was loaded successfully onto the surface of the Mg-amino-clay.

**XRD and FTIR spectra analysis.** Structurally, Mg-amino-clay is a type of 2:1 trioctahedral silicate (Wang et al., 2017). From XRD patterns of Mg-amino-clay and Mg-clay-lipase (Fig. 3a), the typical  $d_{001}$  spacing of Mg-amino-clay was calculated to be 1.68 nm ( $5.25^\circ 2\theta$ ), which is typical for a



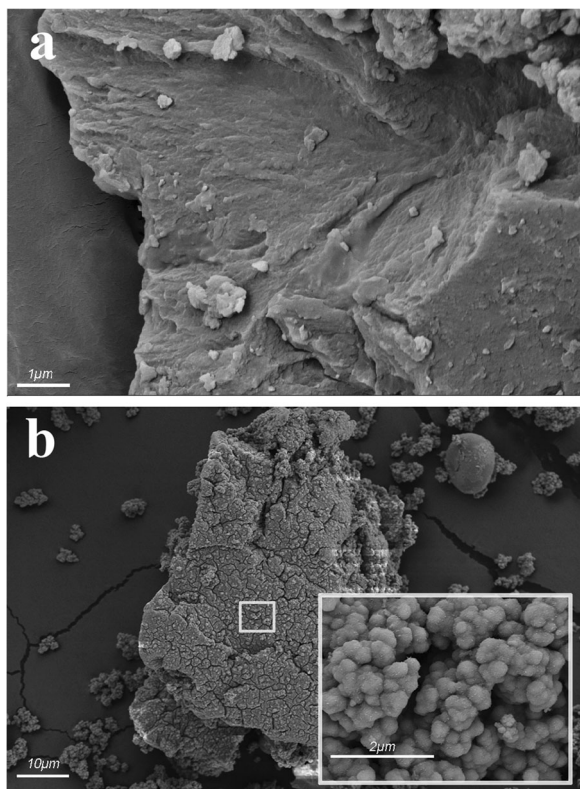


**Fig. 2.** SEM images of **a** Mg-amino-clay and **b** Mg-clay-lipase

layered organo clay (Park et al., 2018). The characteristic ( $d_{020,110}$  and  $d_{130,200}$ ) reflection at  $22^\circ 2\theta$  and the characteristic ( $d_{060}$ ) reflection at  $36^\circ 2\theta$  confirmed the formation of the 2:1 trioctahedral Mg-phyllsilicate clay with a talc-like structure (Datta et al., 2013). The characteristic reflection of the Mg-clay-lipase sample was the same as that of the Mg-amino-clay, so the layer spacing was unaffected by lipase adsorption, which confirmed that the distinctive structure of the Mg-amino-clay was retained. A likely reason was the intercalation of some amino acid residues of lipase while the polypeptide backbone of lipase remained outside of the Mg-amino-clay interlayer space (Sugunan & Gopinath, 2007).

FTIR spectroscopy is a universal technique for determining the secondary structures of proteins. The FTIR spectra of free lipase, Mg-amino-clay, and Mg-clay-lipase (Fig. 3b) provided evidence for the immobilization of lipase on Mg-amino-clay. The amide bond ( $-\text{CO}-\text{NH}-$ ) consists of  $-\text{COOH}$  groups from lipase and  $-\text{NH}_2$  groups from the Mg-amino-clay layer (Patil et al., 2005), indicating a chemical (covalent) bond to immobilize the lipase on the Mg-amino-clay. Four absorption bands were characteristic of the Mg-amino-clay, at  $984\text{ cm}^{-1}$  ( $\text{Si}-\text{O}-\text{Si}$  bending vibration),  $1498\text{ cm}^{-1}$  ( $-\text{CH}_2$  bending vibration),  $1626\text{ cm}^{-1}$  ( $-\text{NH}_2$  bending vibration), and  $1989\text{ cm}^{-1}$  ( $-\text{NH}_2$  stretching vibration). Lipase showed three characteristic bands, at  $3430\text{ cm}^{-1}$  ( $\text{N}-\text{H}$  stretching vibration),  $2974\text{ cm}^{-1}$  and  $2921\text{ cm}^{-1}$  ( $-\text{CH}_2$  stretching vibration), and  $1637\text{ cm}^{-1}$  ( $\text{C}=\text{O}$  stretching vibration, which is also where the amide peak should appear) (Li et al., 2012). The amide band at  $1639\text{ cm}^{-1}$  also appeared in the spectrum

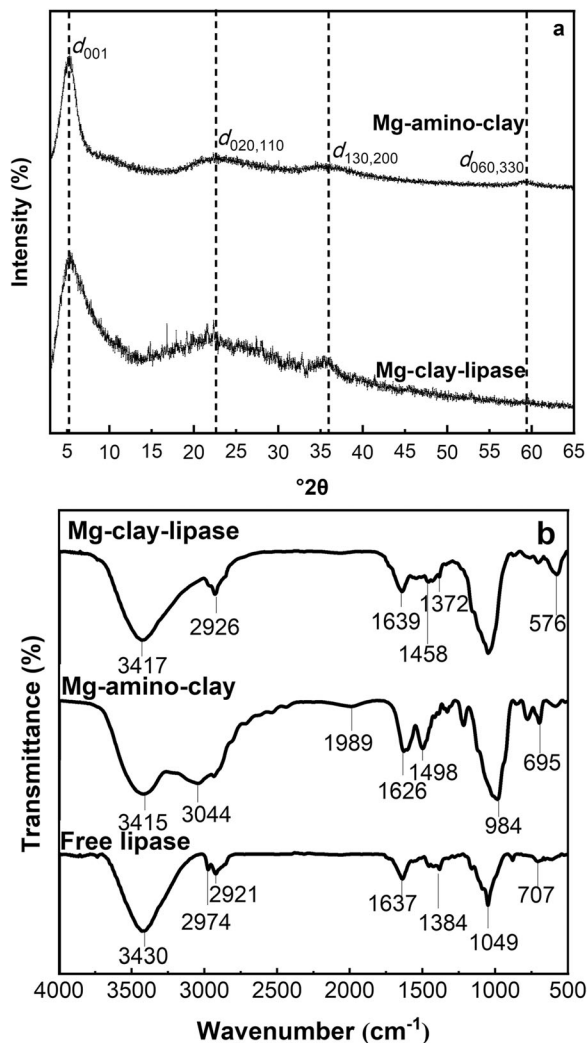


**Fig. 3.** **a** XRD patterns of Mg-amino-clay and Mg-clay-lipase, and **b** FTIR spectra of free lipase, Mg-amino-clay, and Mg-clay-lipase

of Mg-clay-lipase, confirming that the lipase had been immobilized on Mg-amino-clay via the covalent amide bond.

**$\zeta$  potential analysis.** Zeta potential is a significant parameter for reflecting the electrostatic interactions and stability of nanoparticles in aqueous solution. The larger the absolute value of  $\zeta$ , the greater the dispersibility of the solution, so the system is more stable. Zeta potential analyses of free lipase, Mg-amino-clay, and Mg-clay-lipase under various pH values (Fig. 4) suggested that the potential of free lipase was negative, and that the absolute value increased with increase in pH. Mg-amino-clay had a positive potential because of the high density of  $-\text{NH}_4^+$ , and the absolute value increased first and then decreased.  $\zeta$  for Mg-clay-lipase was negative, and the absolute value increased with pH, indicating that the surface of Mg-amino-clay was loaded with negatively charged lipase, resulting in the absolute value of negative potential increasing. Mg-amino-clay showed more stable dispersion in aqueous

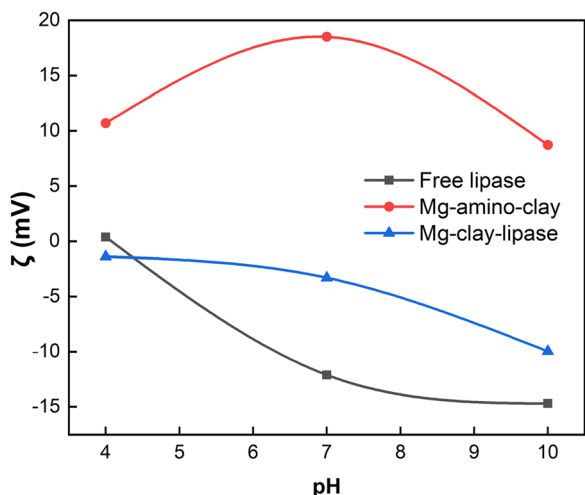


**Fig. 4.** Zeta ( $\zeta$ ) potential analysis of free lipase, Mg-amino-clay, and Mg-clay-lipase

solution compared with free lipase at pH 4 and pH 7. The reason for this was that a large amount of  $-\text{NH}_4^+$  between the layers produced electrostatic repulsion after the Mg-amino-clay was stripped into a single layer in aqueous suspension (Park et al., 2018).

#### Process for Immobilization of Lipase on Mg-amino-clay

The immobilization of lipase on Mg-amino-clay is generally considered to be by interfacial adsorption onto the amphiphilic surface of the clay, which may vary depending on adsorbate-adsorbate interactions. The relative catalytic activity of the Mg-clay-lipase increased as the amount of initial lipase increased up to 70 mg of lipase, and then increased no further above this amount (Fig. 5a). The leveling off must have been due to intermolecular interactions among lipase molecules as its density on the surface increased, thus preventing the exposure of further catalytic sites. 70 mg was, therefore, considered to be the optimum initial dosage of lipase. These results are consistent with other studies (Tudorache et al., 2012; Liu et al., 2013).

The effect of EDC concentration on the interaction of lipase and Mg-amino-clay was also measured (Fig. 5b). The results indicated that the EDC molecules were insufficient to activate  $-\text{COOH}$  for binding lipase below the optimum EDC concentration of 0.6 g/L. On the other hand, excessive use of EDC produced derivatives or released various functional groups, which changed the microenvironment around the carrier, thereby destroying the structure of the lipase or weakening the binding between lipase and the Mg-amino-clay.

The effect of varying reaction time from 1 h to 6 h on the interaction of lipase and Mg-amino-clay was examined further (Fig. 5c). The formation of amide groups between Mg-amino-clay and lipase was observed to be a time-consuming process, with the relative activity of Mg-clay-lipase peaking at 4 h. The relative activity of Mg-clay-lipase increased with reaction time up to 4 h and decreased afterwards. The cause was that the binding sites on Mg-amino-clay by lipase molecules reached

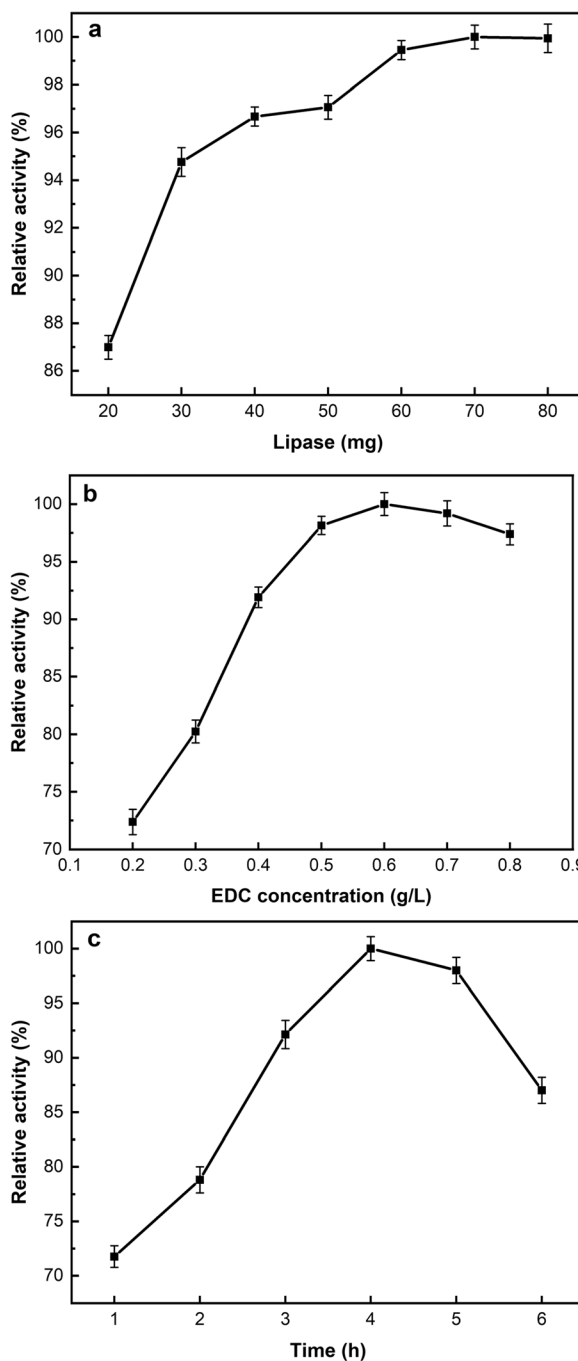


**Fig. 5.** Optimization conditions for lipase immobilization on Mg-amino-clay: **a** the amount of initial lipase, **b** EDC concentration, and **c** reaction time

saturation at 4 h. Enzyme activity decreased after this time due to denaturation. Finally, 4 h was chosen as the optimal immobilization time.

The enzymatic properties of Mg-clay-lipase prepared by EDC and the simple mixture of Mg-amino-clay and lipase under the optimal conditions were investigated to evaluate the effect of the amido bond between Mg-amino-clay and

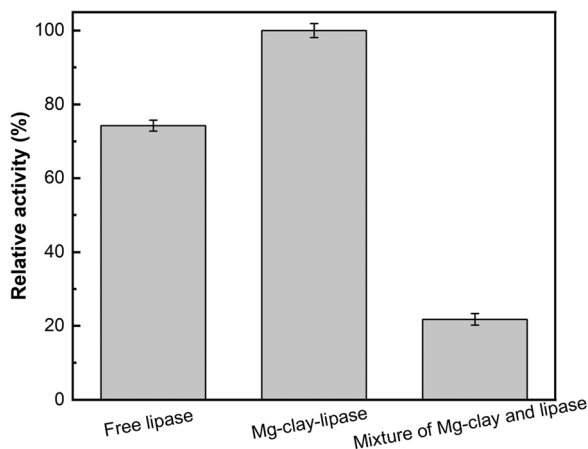


**Fig. 6.** Enzymatic activity of Mg-clay-lipase and of a mixture of Mg-amino-clay and lipase

lipase (Fig. 6). The results suggested that the relative activity of free lipase was 74% of Mg-clay-lipase, while that of the simple mixture was only 22% of Mg-clay-lipase. The reason was that the lipase in the simple mixture was adsorbed on the Mg-amino-clay by electrostatic adsorption, which is very weak, resulting in a dramatic loss of lipase during centrifugation. On the other hand, the immobilized lipase adhered tightly to the surface of Mg-amino-clay by an amide bond with EDC.

#### Enzymatic Activities of Free Lipase and Mg-clay-lipase

Temperature is one of the parameters which affects enzymatic activity. The activities of free lipase and Mg-clay-lipase were evaluated in the range of ~20–60°C (Fig. 7a). The optimum temperature for Mg-clay-lipase was 10°C greater than that for free lipase. The reason was due to the carrier having an obvious effect on the conformational stability of lipase. Immobilization of lipase improved the rigidity of the three-dimensional structure and the stability of the lipase, reducing the influence of temperature on the lipase activity. Mg-clay-lipase required a greater activation energy to rearrange it into a suitable conformation and to form a lipase-substrate complex (Yong et al., 2008), so the optimal reaction temperature was necessarily greater. In addition, the heat energy of the substrate increased with the increase in temperature, and the collision rate of the substrate molecules with the enzyme also increased, causing the improvement in lipase activity as a result. Excessive temperature would destroy the advanced structure of the lipase protein, however, resulting in enzyme inactivation.

pH is a critical parameter in enzymatic catalysis (Badoicdalfard et al., 2019). The activities of free lipase and Mg-clay-lipase were examined from pH 7 to pH 10 (Fig. 7b). The optimum pH for free lipase was ~8.0, while that of Mg-clay-lipase was 8.5, and the stability of Mg-amino-clay was greater than that of free lipase. The higher optimum pH for Mg-clay-lipase was attributed to the anions and cations dissociated by the amino and carboxyl groups in Mg-clay-lipase, which played a role in regulating the acid-base balance of the reaction

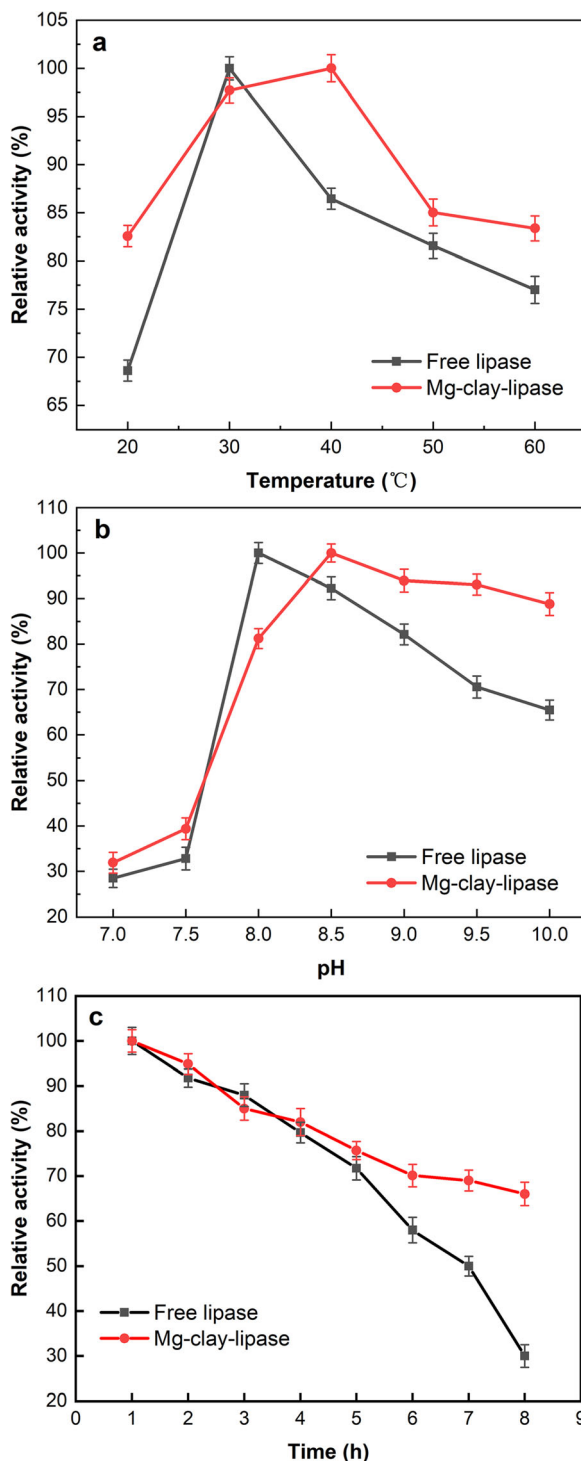


**Fig. 7.** Effect of **a** reaction temperature, **b** reaction pH, and **c** thermal stability at 60°C on enzymatic activity of free lipase and Mg-clay-lipase

system, thus reducing the negative effect of a strong acid or base system on the structure of lipase.

The thermal stabilities of free lipase and Mg-clay-lipase were investigated after incubation at 60°C for 8 h (Fig. 7c). The results showed that the enzyme activity of free lipase preserved

**Table 1.** Kinetic parameters of free lipase and Mg-clay-lipase

Sample	Fitting equation	$v_{\max}$ (mM/(mL·min))	$K_m$ (mM)	$R^2$
Free lipase	$1/v = 0.1718/[S] - 0.0327$	30.58	5.25	0.9984
Mg-clay-lipase	$1/v = 0.1328/[S] - 0.0179$	55.87	7.42	0.9970

only ~30% of the initial activity in the 8<sup>th</sup> hour, while Mg-clay-lipase preserved 80% of the initial activity. This significant result was associated with the multipoint interactions between lipase and Mg-amino-clay which strengthened the intramolecular force and avoided the autolysis of lipase (Zhu et al., 2016).

A series of experiments revealed that the support was helpful for enzyme activity. Lipase is a special ester bond hydrolase with hydrophilic and hydrophobic ends. The active site of lipase was located at the hydrophobic end (Palomo et al., 2007), covered by a “lid,” which is a movable region of the enzyme molecule. Interaction with a hydrophobic phase could lead to the opening of the lid to make the active site accessible; this phenomenon is referred to as “interfacial activation” (Brzozowski et al., 1991; Liu et al., 2020). Because interfacial activation could cause a dramatic increase in catalytic activity, the structure of lipase could be reasonably regulated by constructing a hydrophobic carrier or microenvironment so that the catalytic activity of lipase would be improved. The ATPES provided a large amount of  $-NH_2$  during the construction of the Mg-amino-clay, and the Mg-amino-clay would disperse into single layers in aqueous suspension. On the other hand, the hydrophobic alkane group ( $-CH_2-$ ) could make the Mg-amino-clay hydrophobic. When lipase was loaded onto the hydrophobic supports via covalent bonding, the hydrophobic microenvironment on the carrier made the lid stay open, leading to improvement in the enzymatic activity. As illustrated above, interface activation was the primary cause of enzymatic activity and of improving the tolerance of lipase to immobilization. The activity and

thermostability of lipase could be changed by modifications of their lid domains (Rehm et al., 2010). Furthermore, improving enzyme stability after immobilization could be ascribed to rigidification of enzyme conformation which inhibited protein unfolding (Mehrasbi et al., 2017).

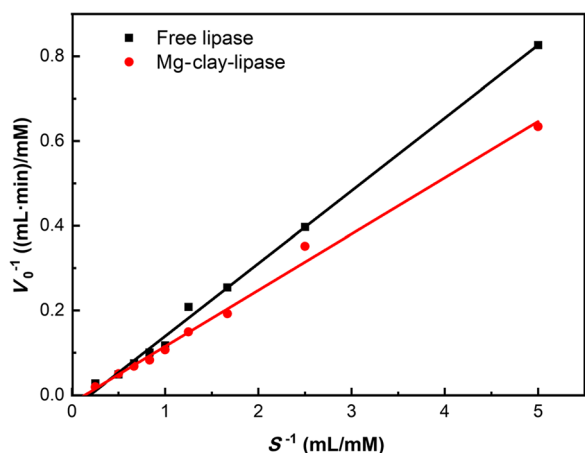
The kinetic parameters of free lipase and Mg-clay-lipase were investigated by calculating initial reaction rates with different substrate concentrations. The kinetics of free lipase and Mg-clay-lipase were assayed for their Michaelis-Menten constant ( $K_m$ ) and maximum reaction rate ( $v_{\max}$ ) (Table 1), which were calculated from Lineweaver-Burk plots using the initial rate of the reaction (Fig. 8). In the case of free lipase, the smaller  $K_m$  value observed indicated a greater lipase affinity for the p-NPP. The main reason was that the presence of the carrier increased the steric hindrance around the lipase and increased the binding resistance between the substrate and the active center of the enzyme protein molecule on the carrier, thus reducing the affinity between the substrate and the enzyme and increasing the  $K_m$  value. On the contrary, the maximum reaction rate,  $v_{\max}$ , of Mg-clay-lipase was greater than that of free lipase, indicating that Mg-clay-lipase had greater catalytic ability due to the increase in Mg-clay-lipase activity under the same conditions. To achieve the same catalytic effect, the Mg-clay-lipase required less time.

## CONCLUSIONS

In the current study, a nanostructured lipase catalyst (Mg-clay-lipase) was synthesized by a covalent cross-linking method using talc-like magnesium amino clay (Mg-amino-clay) as the carrier. The optimal conditions for lipase immobilization included 70 mg of lipase, 0.6 g/L of EDC, and a reaction time of 4 h. The enzymatic activities assay indicated that the optimum reaction temperature of Mg-clay-lipase was 10°C higher than that of free lipase, and Mg-clay-lipase was more stable over a wide pH range; the thermal stability of Mg-clay-lipase was greater than that of free lipase under the optimal conditions. This research provided a new type of nanostructured lipase catalyst and infers that the excellent catalytic performance could be of great industrial value.

## ACKNOWLEDGMENTS

This study was funded by the National Natural Science Foundation of China (NSFC, grant number 42061134018, 42011530085), the Russian Foundation for Basic Research (RFBR, grant number 20-55-53019), and by the Sichuan Science and Technology Program (grant number 2019JDJQ0056).

**Fig. 8.** Lineweaver-Burk plots of free lipase and Mg-clay-lipase



## Funding

Funding sources are as stated in the Acknowledgments.

## Declarations

## Conflict of Interest

The authors declare that they have no conflict of interest.

## REFERENCES

- Aghaei, H., Ghavi, M., Hashemkhani, G., & Keshavarz, M. (2020). Utilization of two modified layered doubled hydroxides as supports for immobilization of *Candida rugosa* lipase. *International Journal of Biological Macromolecules*, *162*, 74–83. <https://doi.org/10.1016/j.ijbiomac.2020.06.145>.
- Akash, A., & Weatherley, L. R. (2018). The performance of microbial lipase immobilized onto polyolefin supports for hydrolysis of high oleate sunflower oil. *Process Biochemistry*, *68*, 100–107.
- Atıroğlu, V. (2020). Lipase immobilization on synthesized hyaluronic acid-coated magnetic nanoparticle-functionalized graphene oxide composites as new biocatalysts: Improved reusability, stability, and activity. *International Journal of Biological Macromolecules*, *145*, 456–465. <https://doi.org/10.1016/j.ijbiomac.2019.12.233>.
- Badoei-dalfard, A., Malekabadi, S., Karami, Z., & Sargazi, G. (2019). Magnetic cross-linked enzyme aggregates of Km12 lipase: A stable nanobiocatalyst for biodiesel synthesis from waste cooking oil. *Renewable Energy*, *141*, 874–882.
- Barse, L. Q., Graebin, N. G., Cipolatti, E. P., Robert, J. M., Pinto, M. C. C., Pinto, J. C. C. S., et al. (2019). Production and optimization of isopropyl palmitate via biocatalytic route using home-made enzymatic catalysts. *Journal of Chemical Technology & Biotechnology*, *94*, 389–397.
- Bradford, M. M. (1976). A rapid and sensitive method for the quantitation of microgram quantities of protein utilizing the principle of protein-dye binding. *Analytical Biochemistry*, *72*, 248–254. <https://doi.org/10.1006/abio.1976.9999>.
- Brzozowski, A. M., Derewenda, U., Derewenda, Z. S., Dodson, G. G., Lawson, D. M., Turkenburg, J. P., et al. (1991). A model for interfacial activation in lipases from the structure of a fungal lipase-inhibitor complex. *Nature*, *351*, 491–494. <https://doi.org/10.1038/351491a0>.
- Burkett, S. L., Press, A., & Mann, S. (1997). Synthesis, characterization, and reactivity of layered inorganic-organic nanocomposites based on 2:1 trioctahedral phyllosilicates. *Chemistry of Materials*, *9*, 1071–1073.
- Cipolatti, E. P., Manoel, E. A., Fernandez-Lafuente, R., & Freire, D. M. G. (2017). Support engineering: relation between development of new supports for immobilization of lipases and their applications. *Biotechnology Research and Innovation*, *1*, 26–34.
- Datta, K. K. R., Achari, A., & Eswaramoorthy, M. (2013). Aminoclay: a functional layered material with multifaceted applications. *Journal of Materials Chemistry*, *1*(6707), 6718. <https://doi.org/10.1039/c3ta00100h>.
- de Barros, D. S. N., Fernandez-Lafuente, R., Aguiéiras, E. C. G., & Freire, D. M. G. (2019). Production of lipases in cottonseed meal and application of the fermented solid as biocatalyst in esterification and transesterification reactions. *Renewable Energy*, *130*, 574–581.
- de Paula, A. V., dos Santos, J. C., Nunes, G. F. M., & de Castro, H. E. (2018). Performance of packed bed reactor on the enzymatic interesterification of milk fat with soybean oil to yield structure lipids. *International Dairy Journal*, *86*, 1–8.
- Fernandez-Lafuente, R., Armisén, P., Sabuquillo, P., Fernández-Lorente, G., & Guisán, J. M. (1998). Immobilization of lipases by selective adsorption on hydrophobic supports. *Chemistry and Physics of Lipids*, *93*, 185–197. [https://doi.org/10.1016/s0009-3084\(98\)00042-5](https://doi.org/10.1016/s0009-3084(98)00042-5).
- Gupta, M. N., Jain, P., & Jain, S. (2005). A microwave-assisted microassay for lipases. *Analytical and Bioanalytical Chemistry*, *381*, 1480–1482.
- Hanefeld, U., Gardossi, L., & Magner, E. (2009). Understanding enzyme immobilisation. *Chemical Society Reviews*, *38*, 453–468. <https://doi.org/10.1039/b711564b>.
- Hartmann, M., & Kostrov, X. (2013). Immobilization of enzymes on porous silicas – benefits and challenges. *Chemical Society Reviews*, *42*, 6277–6289. <https://doi.org/10.1039/c3cs60021a>.
- Holmström, S., Patil, A. J., Butler, M., & Mann, S. (2007). Influence of polymer co-intercalation on guest release from aminopropyl-functionalized magnesium phyllosilicate mesolamellar nanocomposites. *Journal of Materials Chemistry*, *17*, 3894–3900.
- Kavadia, M. R., Yadav, M. G., Odaneth, A. A., & Lali, A. M. (2018). Synthesis of designer triglycerides by enzymatic acidolysis. *Biotechnol Rep (Amst)*, *18*, e00246. <https://doi.org/10.1016/j.btre.2018.e00246>.
- Kołodziejaska, R., Studzińska, R., & Pawluk, H. (2018). Lipase-catalyzed enantioselective transesterification of prochiral 1-((1,3-dihydroxypropan-2-yl)oxymethyl)-5,6,7,8-tetrahydroquinazolin-2,4(1H,3H)-dione in ionic liquids. *Chirality*, *30*, 206–214. <https://doi.org/10.1002/chir.22787>.
- Li, Y., Li, J., & Dong, H. (2012). Improvement of catalytic activity and stability of lipase by immobilization on organobentonite. *Chemical Engineering Journal*, *181–182*, 590–596.
- Liu, D. M., Chen, J., & Shi, Y. P. (2018a). Advances on methods and easy separated support materials for enzymes immobilization. *Trends in Analytical Chemistry*, *102*, 332–342. <https://doi.org/10.1016/j.trac.2018.03.011>.
- Liu, J., Guo, H., & Zhou, Q. (2013). Highly efficient enzymatic preparation for dimethyl carbonate catalyzed by lipase from *Penicillium expansum* immobilized on CMC-PVA film. *Journal of Molecular Catalysis, B: Enzymatic*, *96*, 96–102.
- Liu, X., Fang, Y., Yang, X., Li, Y., & Wang, C. (2018b). Electrospun epoxy-based nanofibrous membrane containing biocompatible feather polypeptide for highly stable and active covalent immobilization of lipase. *Colloids and Surfaces B: Biointerfaces*, *166*, 277–285. <https://doi.org/10.1016/j.colsurfb.2018.03.037>.
- Liu, J., Ma, R. T., & Shi, Y. P. (2020). "Recent advances on support materials for lipase immobilization and applicability as biocatalysts in inhibitors screening methods" – A review. *Analytica Chimica Acta*, *1101*, 9–22. <https://doi.org/10.1016/j.aca.2019.11.073>.
- Löfgren, J., Görbe, T., Oschmann, M., Svedendahl Humble, M., & Bäckvall, J. E. (2019). Transesterification of a Tertiary Alcohol by Engineered *Candida antarctica* Lipase A. *Chembiochem*, *20*, 1438–1443. <https://doi.org/10.1002/cbic.201800792>.
- Madhavan, A., Sindhu, R., Binod, P., Sukumaran, R. K., & Pandey, A. (2017). Strategies for design of improved biocatalysts for industrial applications. *Bioresource Technology*, *245*, 1304.
- Manoel, E. A., Dos Santos, J. C., Freire, D. M., Rueda, N., & Fernandez-Lafuente, R. (2015). Immobilization of lipases on hydrophobic supports involves the open form of the enzyme. *Enzyme and Microbial Technology*, *71*, 53–57. <https://doi.org/10.1016/j.enzmictec.2015.02.001>.
- Mehrasbi, M. R., Mohammadi, J., Peyda, M., & Mohammadi, M. (2017). Covalent immobilization of *Candida antarctica* lipase on core-shell magnetic nanoparticles for production of biodiesel from waste cooking oil. *Renewable Energy*, *101*, 593–602.
- Öztürk, H., Pollet, E., Phalip, V., Güvenilir, Y., & Avérous, L. (2016). Nanoclays for lipase immobilization: biocatalyst characterization and activity in polyester synthesis. *Polymers*, *8*, 416.
- Palomo, J. M., Fernandez-Lorente, G., & Mateo, C. (2007). Improvement of enzyme activity, stability and selectivity via immobilization techniques. *Enzyme and Microbial Technology*, *40*, 1451–1463.
- Papadaki, A., Fernandes, K. V., Guimaraes Freire, D. M., Koutinas, A. A., Cavalcanti da Silva, J. A., & Fernandez-Lafuente, R. (2018). Enzymatic esterification of palm fatty-acid distillate for the



- production of polyol esters with biolubricant properties. *Industrial Crops and Products*, 116, 90–96.
- Park, D., Lee, Y. C., & Hoang Bui, V. K. (2018). Aminoclays for biological and environmental applications: An updated review. *Chemical Engineering Journal*, 336, 757–772.
- Patil, A. J., Muthusamy, E., & Mann, S. (2005). Fabrication of functional protein–organoclay lamellar nanocomposites by biomolecule-induced assembly of exfoliated aminopropyl-functionalized magnesium phyllosilicates. *Journal of Materials Chemistry*, 15, 3838–3843.
- Patil, A. J., Li, M., Dujardin, E., & Mann, S. (2007). Novel bioinorganic nanostructures based on mesolamellar intercalation or single-molecule wrapping of DNA using organoclay building blocks. *Nano Letters*, 7, 2660–2665.
- Rehm, S., Trodler, P., & Pleiss, J. (2010). Solvent-induced lid opening in lipases: a molecular dynamics study. *Protein Science: A Publication of the Protein Society*, 19, 2122–2130. <https://doi.org/10.1002/pro.493>.
- Sheldon, R. A. (2007). Enzyme immobilization: The quest for optimum performance. *Advanced Synthesis & Catalysis*, 349, 1289–1307.
- Sugunan, S., & Gopinath, S. (2007). Enzymes immobilized on montmorillonite K10: Effect of adsorption and grafting on the surface properties and the enzyme activity. *Applied Clay Science*, 35, 67–75.
- Tudorache, M., Coman, S., & Protesescu, L. (2012). Efficient bioconversion of glycerol to glycerol carbonate catalyzed by lipase extracted from *Aspergillus niger*. *Green Chemistry*, 14, 478–482.
- Urrutia, P., Arrieta, R., Alvarez, L., Cardenas, C., Mesa, M., & Wilson, L. (2018). Immobilization of lipases in hydrophobic chitosan for selective hydrolysis of fish oil: The impact of support functionalization on lipase activity, selectivity and stability. *International Journal of Biological Macromolecules*, 108, 674–686. <https://doi.org/10.1016/j.ijbiomac.2017.12.062>.
- Wang, J., Zhao, G., & Yu, F. (2016). Facile preparation of Fe<sub>3</sub>O<sub>4</sub>@MOF core-shell microspheres for lipase immobilization. *Journal of the Taiwan Institute of Chemical Engineers*, 69, 139–145.
- Wang, R., Jing, G., Zhou, X., & Lv, B. (2017). Removal of chromium(VI) from wastewater by Mg-aminoclay coated nanoscale zero-valent iron. *Journal of Water Process Engineering*, 18, 134–143.
- Wang, K., Sun, S., Ma, B., Dong, F., Huo, T., Li, X., & 3 others (2019). Construction and characterization of a nanostructured biocatalyst consisting of immobilized lipase on aminopropyl-functionalized montmorillonite. *Applied Clay Science*, 183, 105329.
- Wijnants, M., Cornet, I., & Bauwelinck, J. (2018). Investigation of the enzyme-catalysed transesterification of methyl acrylate and sterically hindered alcohol substrates. *Chemistry Select*, 3, 1–7.
- Yong, Y., Bai, Y., Li, Y., Lin, L., Cui, Y., & Xia, C. (2008). Characterization of *Candida rugosa* lipase immobilized onto magnetic microspheres with hydrophilicity. *Process Biochemistry*, 43, 1179–1185.
- Zhu, W., Zhang, Y., Hou, C., Pan, D., He, J., & Zhu, H. (2016). Covalent immobilization of lipases on monodisperse magnetic microspheres modified with PAMAM-dendrimer. *Journal of Nanoparticle Research*, 18, 13.

(Received 27 August 2020; revised 7 April 2021; Guest AE: Nithima Khaorapong)